Thermochimica Acta, 224 (1993) 19–32
Elsevier Science Publishers B.V., Amsterdam

Thermochemistry and structure of the liquid Na_2O–GeO_2 system

M. Fan, F. Müller * and W. Wilsmann

Institut für Gesteinshüttenkunde, Rheinisch-Westfälische Technische Hochschule Aachen, Mauerstr. 5, D-52056 Aachen (Germany)

(Received 3 February 1993; accepted 5 February 1993)

Abstract

The integral molar enthalpy of mixing of the liquid mixture Na_2O–GeO_2 was measured in the composition range from 15 to 100 mol.% GeO_2 at 1400 K by the drop-mixing method using a differential high-temperature integrated heat-flux calorimeter. The partial molar enthalpies of mixing of the component oxides were obtained by the method of intercepts. The enthalpies of mixing are exothermic at all compositions. Near $x_{GeO_2} \approx 0.33$, the integral enthalpy shows a minimum value ($\Delta_m H = -134\,kJ\,mol^{-1}$), and the partial enthalpies display a sharp dependence on composition. The strong energetic asymmetry of the considered system is attributed to the energy associated with the breakdown of the network structure of liquid GeO_2. The relationship between these structural changes and the thermochemical properties of the liquid mixture is discussed, employing a simple electrostatic model and using the information reported on the structures of sodium germanate glasses and melts in the literature.

INTRODUCTION

In a continuation of our previous work [1, 2], we have measured, in the present study, the integral molar enthalpy of mixing of the liquid Na_2O–GeO_2 system at 1400 K by drop-mixing calorimetry. At this temperature, Na_2O is solid (m.p. 1405 K) while GeO_2 is liquid (m.p. 1389 K) and, according to the phase diagram of the Na_2O–GeO_2 system [3–7], the stability region of the liquid mixture Na_2O–GeO_2 covers nearly the entire range of composition.

The main objective of the present investigation is the completion of the thermochemical data base for the Na_2O–GeO_2 system, as well as the provision of systematic experimental data on the thermochemical behaviour of oxide liquids. Though a substantial amount of structural information on sodium germanate glasses and melts has been provided during the last three decades, as will be discussed later, the thermochemical

* Corresponding author.

data base of these materials is still insufficient. The only thermochemical studies known to the authors were primarily directed at the measurement of the partial molar Gibbs energies of the component oxides [8, 9]; values of the partial molar enthalpy and entropy were derived from the temperature dependence of the Gibbs energy. A comparison, however, shows that the results obtained differ considerably.

EXPERIMENTAL

Calorimetric measurements were made by the drop-mixing method. Samples containing well-defined mechanical mixtures of pure Na_2O and hexagonal GeO_2 or of pure Na_2O and vitreous GeO_2 at room temperature were dropped into the calorimeter operating at 1400 K, and the enthalpic effects associated with the reactions occurring in the calorimeter were measured. Details of the method of measurement have been reported in previous publications [1, 2].

All calorimetric experiments were performed in a novel differential high-temperature integrated heat-flux calorimeter. This apparatus, which was recently developed in this laboratory from the Setaram HT 1500 calorimeter, is now produced by Setaram in France and is available commercially under the designation "Multi Detector High-Temperature Calorimeter". The mechanical design of the calorimetric detector used in this calorimeter is mainly based on the construction principles described in detail in a previous publication from this laboratory [10].

The central part of the new calorimeter is represented by the "grooved tube" (length 80 mm; O.D. 20.1 mm; I.D. 17.5 mm) shown in Fig. 1, made from recrystallized alumina. In the wall of the tube, 60 grooves (width 0.5 mm; depth 0.5 mm), cut equidistantly from the outer surface, run parallel to the longitudinal axis. The grooves serve to accommodate the leads of a thermopile, as described below. A disc-shaped piece of alumina fixed in the middle of the grooved tube by an alumina bolt divides the space enclosed by the tube into two halves. The upper half, acting as the "working cell" of the differential calorimeter, contains the "working crucible" (I.D. 16.5 mm) in which the sample reacts during a calorimetric measurement. The lower half represents the "reference cell" of the calorimeter and holds the "reference crucible". In the calorimetric measurements performed in the course of this study, both the working and reference crucibles were lined by a platinum crucible in order to protect the alumina working crucible from attack by the samples and to maintain a constant and uniform temperature in the reference cell.

Temperature differences between the working and reference cells are measured by a thermopile composed of 58 thermocouples made from 0.5 mm Pt/Pt–Rh10 wires. The thermocouples are inter-connected in series, and couples allocated to the working cell alternate with couples assigned to

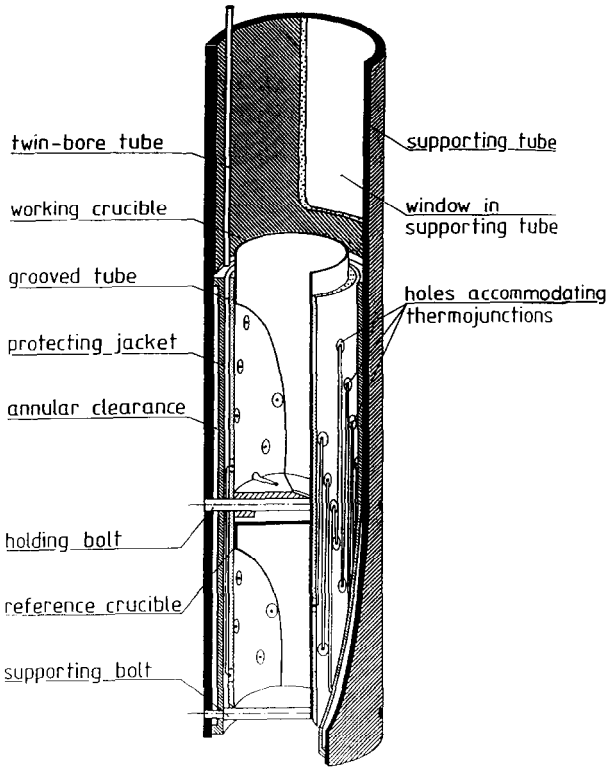

Fig. 1. Diagrammatic representation of the detector employed in the Setaram Multi-Detector High-Temperature Calorimeter. The grooves on the outside surface of the grooved tube, the charging tube through which samples are dropped into the working crucible, and the lid closing this crucible are not shown. The ceramic parts of the calorimetric detector are made from recrystallized α-alumina.

the reference cell. Hence, each cell possesses 28 thermojunctions, from which 24 junctions are fixed in holes regularly arranged at five levels, about 8 mm apart, over the wall of the grooved tube, while the remaining 4 junctions are distributed over the bottom of the crucible. Thus, for each thermojunction in the working cell, a mirror-inverted counterpart exists in the reference cell. Along the wall of the grooved tube, the thermocouple leads run through the grooves which establish the connections between corresponding holes in the tube; the leads are held in position by the protecting jacket which tightly encloses the grooved tube. The jacket is in turn surrounded by the supporting tube; the radial clearance between the jacket and this tube has a constant width of about 0.75 mm. Above the working crucible, two windows, opposing each other, have been cut in the supporting tube through which a crucible, held by the working cell, can be removed and replaced if needed.

Samples are introduced from the outside into the working cell through

an alumina tube ("charging tube" not shown in Fig. 1) projecting into the working crucible. The ring slot between the crucible and the charging tube is closed by a ring-like alumina lid (not shown in Fig. 1). The temperature of the calorimeter is measured by a Pt/Pt–Rh10 thermocouple, the hot junction of which is located at the bottom of the working crucible. The end leads of the thermopile and the leads of the thermocouples reading the calorimeter and furnace temperatures run through the bores of twin-bore alumina tubes to a plug socket from where the measured values are fed into a data processing system, described below.

By means of the supporting tube, the calorimeter is suspended in an alumina tube (I.D. 23 mm) which is in turn surrounded by a graphite tube; this tube system is mounted in a water-cooled vacuum jacket. The graphite tube acts as a heating element which, due to its special profile, allows a zone of constant temperature to be established around the detector.

In order to process the data obtained during the calorimetric measurements (the voltage of the thermopile and that of the thermocouples measuring the calorimeter and furnace temperatures), the microprocessor-operated Setaram G 11 controller is first employed; this amplifies, digitizes, and, finally, transfers the data via an RS 232 series interface to an IBM compatible computer which evaluates the information provided by the measurements. The Setaram G 11 controller is also used to control the furnace temperature, while thyristors are employed to adjust the electric power fed into the graphite heating tube. The electric power is stabilized by an electronic A.C.-voltage stabilizer (Philips PE 1605).

Before initiating an experiment, the vacuum jacket and the calorimeter chamber were evacuated by a single-stage rotary pump; during a measurement, they were flushed with argon gas (purity 99.9998 vol.%; flow rate 0.5 $cm^3 s^{-1}$). The calibration of the calorimeter was performed by dropping spheres of platinum at room temperature into the calorimeter operating at the measurement temperature. The enthalpy effects in the calibrations were calculated using Kelley's enthalpy data for platinum [11].

Pure crystalline disodium oxide was prepared from NaN_3 (purissimum; Merck, Darmstadt, Germany) and $NaNO_3$ (optipur; Merck, Darmstadt, Germany) according to the reaction

$$5NaN_3 + NaNO_3 = 3Na_2O + 8N_2 \quad (1)$$

using the method described by Zintl and von Baumbach [12]. The Na_2O thus obtained was transferred in batches of 250 mg under vacuum to a glove box in which an atmosphere free from H_2O and CO_2 was maintained; the material was stored here in a desiccator until use. Examination of the substance by X-ray diffraction employing Cu Kα radiation detected well-crystallized single-phase Na_2O.

Germanium dioxide was employed as hexagonal GeO_2 and as germania glass. The hexagonal GeO_2 had a purity of 99.999 mass% (Fluka, Buchs,

Switzerland). Germania glass was prepared by heating batches of hexagonal GeO_2 at about 1550 K for 20 h in a platinum crucible in air and by casting the melt onto a cold silver plate. X-ray powder diffraction and microscopic examination confirmed hexagonal GeO_2 and a single-phase glass. Both substances were ground in a ball mill; the powders were sieved, and the fractions with a particle size below 20 μm were stored for calorimetry. Prior to use, both fine GeO_2 powders were annealed for 12 H under vacuum (<0.01 Pa) at 800 K in order to remove H_2O and CO_2.

From the fine powders of the component oxides, two-phase mixtures, $Na_2O + GeO_2$(hex) and $Na_2O + GeO_2$(glass) of defined composition, were prepared in the glove box. To this end, required amounts of the oxides were weighed out and intimately mixed in a mixer mill (with three-dimensional motion for colloidal micro-grinding and homogeneous mixing). From the mixtures thus prepared, quantities of about 40 mg were placed in small platinum capsules and compacted therein. The capsules made from 10 μm foil weighed about 15 mg. The enthalpy effects caused by the capsules in the calorimetric measurements were determined from Kelley's enthalpy data [11].

In order to protect the samples from water and carbon dioxide in the air, they were taken individually from the glove box to the calorimeter, using the sample holder described below. When this holder had been connected to the charging tube of the calorimeter by a ground-glass joint, and this latter tube and the calorimeter had been flushed using argon gas, the sample was dropped from the sample holder into the calorimeter in order to start the experiment.

The main part of the sample holder, Fig. 2, consists of a glass tube enlarged spherically in the middle. The sample is introduced into this spherical part through a side arm which is closed by a ground-glass stopper. The spherical part is sealed above and below by O-rings mounted on a glass rod. The sample is released from the holder by lifting the glass rod.

RESULTS AND DISCUSSION

Calorimetric measurements have been made in the composition range $0.15 < x < 1$, where x signifies the mole fraction of GeO_2 in the mixture Na_2O–GeO_2. The results are given in Table 1 and are plotted versus composition in Fig. 3. Measurements were not made in the range below $x = 0.15$, in order to avoid corrosive attack of the ceramic parts of the calorimeter by Na_2O vaporizing from Na_2O-rich samples. Therefore, the enthalpy change of the reaction

$$Na_2O(sol, 296\,K) \rightarrow Na_2O(liq, 1400\,K) \quad (2)$$

had to be taken from the literature [13]

$$H(1400\,K) - H(296) = 160.63\ kJ\ mol^{-1} \quad (3)$$

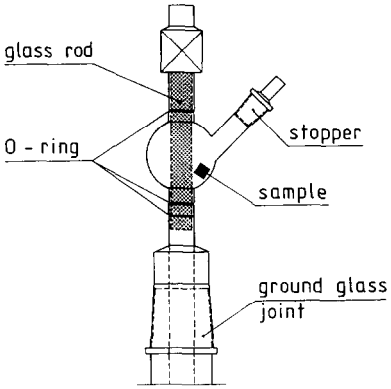

Fig. 2. Sample holder attached by means of a ground-glass joint to the upper end of the charging tube.

when the integral molar enthalpy of mixing $\Delta_m H$ was calculated from the data listed in Table 1. The enthalpies of mixing thus obtained for 1400 K are given in Table 2 and are represented in Fig. 4 as a function of x. The partial molar enthalpies of mixing, $\Delta\bar{H}_{Na_2O}$ and $\Delta\bar{H}_{GeO_2}$, of Na_2O(liq) and GeO_2(liq), respectively, in the liquid mixture Na_2O–GeO_2 were determined by the method of intercepts, i.e. by drawing tangents to a larger scale graph of $\Delta_m H$ versus mole fraction; the data valid for 1400 K are shown as curves in Fig. 5.

The data depicted in Figs. 4 and 5 may first be compared with corresponding information from the literature. Using the Knudsen method in combination with a mass-spectrometric analysis of the vapour effusing from the Knudsen cell, Shul'ts et al. [9] measured the partial molar Gibbs energies of the oxide components of the liquid mixture Na_2O–GeO_2 in the composition range $0.5 < x < 1$, at temperatures between 1490 and 1550 K, and, from the temperature dependence of the partial Gibbs energies, they determined the corresponding partial enthalpies and entropies. As a result of this investigation, the values of the integral molar Gibbs energy, enthalpy, and entropy of mixing of the liquid system Na_2GeO_3–GeO_2 were reported for 1543 K in graphical form using Na_2GeO_3(liq) and GeO_2(liq) as reference states, whereas the enthalpy of mixing values reported in the present study are related to pure liquid Na_2O and GeO_2. For the purpose of comparison, the enthalpy data of Shul'ts et al. [9] have therefore been converted into values related to the pure liquid components. In doing so, the integral molar enthalpy of mixing at $x = 0.5$ has been taken from the data plotted in Fig. 4: $\Delta_m H = -118.4\ \text{kJ mol}^{-1}$. On the basis of this value, the data represented by the broken line in Fig. 4 have been calculated.

Employing a solid-electrolyte concentration cell of the type

$$Pt,O_2 \mid (1-x)Na_2O \cdot xGeO_2 \parallel \alpha - Al_2O_3 \parallel 0.1Na_2O \cdot 0.9GeO_2 \mid O_2,Pt$$

TABLE 1

Enthalpy increment $H(1400\,K) - H(295\,K)$ measured by heating GeO_2(hex), GeO_2(glass), and mixtures of $Na_2O + GeO_2$(hex) and of $Na_2O + GeO_2$(glass) in the calorimeter from room temperature (296 K) to the calorimetric temperature (1400 K). Composition of mixtures is given by the mole fraction x of GeO_2; figures in parentheses denote the number of individual measurements

x_{GeO_2}	$H(1400\,K) - H(296\,K)/(kJ\,mol^{-1})$	
	$Na_2O + GeO_2$(hex)	$Na_2O + GeO_2$(glass)
0.15		70.05 ± 4.0 (4)
0.20	51.30 ± 3.0 (4)	
0.25		26.78 ± 3.0 (5)
0.275		15.51 ± 1.5 (5)
0.30	9.21 ± 1.5 (4)	
0.315		2.28 ± 0.5 (7)
0.33	4.38 ± 3.0 (4)	
0.35		−1.34 ± 1.5 (4)
0.375	9.02 ± 1.0 (5)	
0.40	2.62 ± 1.5 (4)	
0.425		−3.60 ± 2.5 (6)
0.45	8.17 ± 0.5 (4)	
0.50	9.10 ± 3.0 (3)	
0.525		3.90 ± 0.5 (8)
0.55		6.14 ± 3.0 (5)
0.575	17.89 ± 2.5 (4)	
0.60	20.53 ± 3.0 (4)	
0.625		13.64 ± 2.0 (4)
0.65	26.90 ± 3.0 (4)	
0.70	33.31 ± 0.3 (5)	
0.75	42.67 ± 1.5 (6)	31.55 ± 3.0 (4)
0.80	50.98 ± 1.0 (5)	
0.825		40.72 ± 1.5 (5)
0.875		50.66 ± 0.5 (7)
0.90	71.64 ± 2.0 (5)	
0.925		62.47 ± 3.0 (4)
0.95		67.46 ± 3.5 (5)
1.00	94.28 ± 2.5 (5)	77.70 ± 1.0 (8)

Kohsaka et al. [8] measured the partial Gibbs energy of Na_2O in Na_2O–GeO_2 melts at compositions from $x = 0.45$ to $x = 1$ and at temperatures between 1350 to 1520 K. From these data, they calculated, on the basis of the Gibbs–Duhem equation, the partial Gibbs energy of GeO_2, and, from the temperature dependence of the partial Gibbs energy, they derived the values of the partial enthalpy and entropy of the component oxides. The thermodynamic data thus obtained refer, respectively, to Na_2O dissolved in a Na_2O–GeO_2 melt containing 10 (or 15) mol.% Na_2O and to liquid GeO_2. In order to convert the enthalpy data of Kohsaka et al. [8]

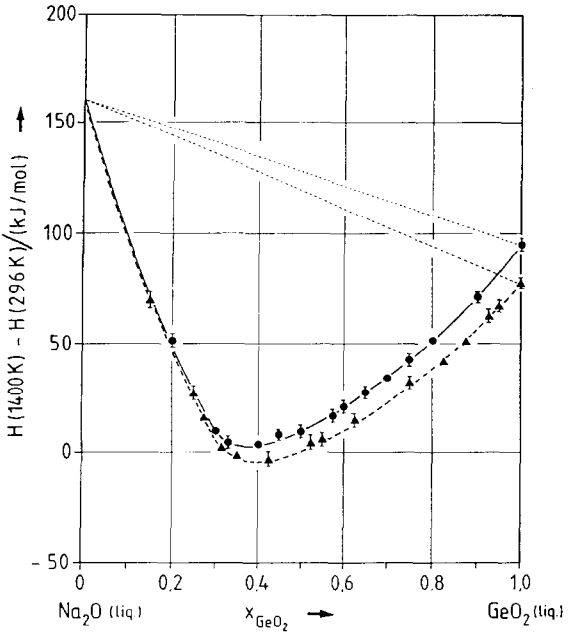

Fig. 3. Enthalpy increments $H(1400\,K) - H(296\,K)$ measured by heating $Na_2O + GeO_2$(hex.) and $Na_2O + GeO_2$(glass) mixtures of defined composition x in the calorimeter from room temperature $T_r = 296\,K$ to the calorimetric temperature $T_c = 1400\,K$: ●, $(1-x)Na_2O + xGeO_2$(hex.); ▲, $(1-x)Na_2O + xGeO_2$(glass).

TABLE 2

Integral molar enthalpy of mixing $\Delta_m H$ of the liquid system Na_2O–GeO_2 at 1400 K as a function of composition given by the mole fraction x of GeO_2; reference states: Na_2O(liq), GeO_2(liq)

x_{GeO_2}	$\Delta_m H$/(kJ mol^{-1})	x_{GeO_2}	$\Delta_m H$/(kJ mol^{-1})
0.15	−78.14 ± 6.0	0.55	−108.88 ± 4.0
0.20	−96.06 ± 5.0	0.575	−104.59 ± 3.5
0.25	−113.12 ± 5.0	0.60	−100.29 ± 5.0
0.275	−122.31 ± 3.0	0.625	−95.16 ± 3.0
0.30	−131.35 ± 3.5	0.65	−90.60 ± 5.0
0.315	−132.23 ± 2.0	0.70	−80.88 ± 2.5
0.33	−134.35 ± 5.0	0.75	−68.20 ± 3.0
0.35	−132.95 ± 3.0	0.75	−66.88 ± 3.5
0.375	−130.99 ± 3.0	0.80	−56.57 ± 3.0
0.40	−131.47 ± 4.0	0.825	−51.49 ± 3.0
0.425	−129.03 ± 3.5	0.875	−37.41 ± 2.0
0.45	−122.60 ± 3.0	0.90	−29.28 ± 4.0
0.50	−118.36 ± 5.0	0.925	−21.45 ± 4.5
0.525	−113.21 ± 2.0	0.95	−14.39 ± 4.5

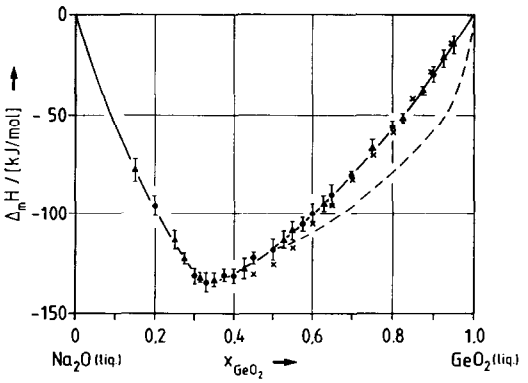

Fig. 4. Integral molar enthalpy of mixing $\Delta_m H$ of the liquid mixture $Na_2O + GeO_2$ as a function of composition expressed by the mole fraction x of GeO_2; standard states: Na_2O(liq), GeO_2(liq): ●, this work from measurements on mixtures of $Na_2O + GeO_2$(hex) at 1400 K; ▲, this work from measurements on mixtures of $Na_2O + GeO_2$(glass) at 1400 K; Shul'ts et al. [9] at 1543 K; ×, Kohsaka et al. [8] at 1450 K.

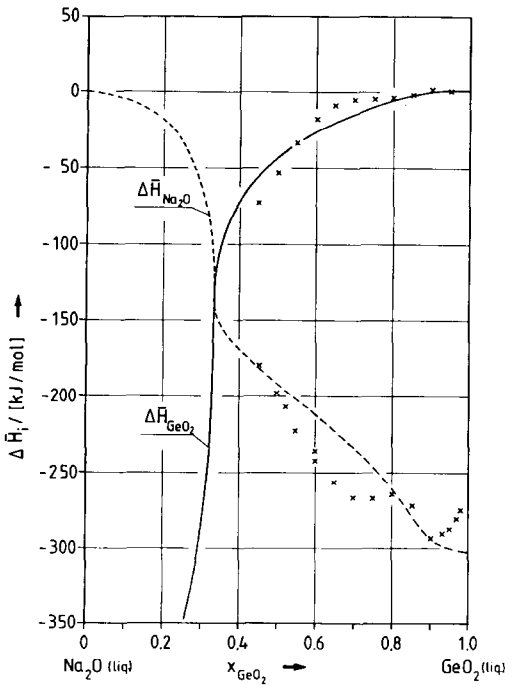

Fig. 5. Partial molar enthalpy of mixing $\Delta \bar{H}_i$ of Na_2O(liq) and GeO_2(liq) in the liquid mixture $Na_2O + GeO_2$ as a function of composition given by the mole fraction x of GeO_2; – – –, this work for Na_2O at 1400 K; —, this work for GeO_2 at 1400 K; ×, Kohsaka et al. [8] at 1450 K.

into values referred to liquid Na_2O and GeO_2, the value of the partial molar enthalpy of solution of liquid Na_2O in a Na_2O–GeO_2 melt containing 10 mol.% Na_2O was taken from the data set plotted in Fig. 5: $\Delta\bar{H}_{Na_2O} = -291$ kJ mol^{-1}. The partial enthalpy values calculated in this way from the results of Kohsaka et al. are shown in Fig. 5.

The comparisons in Figs. 4 and 5 show that the results from Shul'ts et al. [9] are at variance with the findings of the present investigation, while the results from Kosaka et al. [8] are in partial agreement with the data of this study. The discrepancies, which can obviously not be attributed to the temperature differences existing between the individual measurements, do not, however, come as a surprise, as it is well known that enthalpies (and entropies) obtained from the temperature coefficients of Gibbs energies are usually uncertain and are often subject to large errors.

Some significant features emerge from the plots in Figs. 4 and 5. In the vicinity of $x = 0.33$, the integral enthalpy (Fig. 4) exhibits a well-defined minimum and the partial enthalpy (Fig. 5) shows a point of inflection as well as a sharp dependence on composition. Furthermore, it is noted that the enthalpy of mixing curve in Fig. 4 does not possess, within the experimental certainty, a sigmoid shape, as is generally found for liquid mixtures composed of network-forming and network-modifying components (the following systems may serve as examples: LiF–BeF_2, KF–BeF_2 [14], CaO–SiO_2 [15, 16], PbO–SiO_2 [17], BaO–B_2O_3 [2], PbO–B_2O_3 [18]). In contrast, the enthalpy of mixing curve in Fig. 4 exhibits positive curvature over the entire range of composition. Thus, there is no indication of any tendency of the liquid Na_2O–GeO_2 mixtures towards phase separation. This conclusion is in accord with the information available from the phase diagram [4–7]; here the liquidus line displays no point of inflection. It may, however, be mentioned that the GeO_2-saturated liquidus lines in the related Li_2O–GeO_2 and K_2O–GeO_2 systems are S-shaped [19, 20]. In the absence of any indications of a tendency to phase separation, the Na_2O–GeO_2 system turns out to be an apparently exceptional case among the glass-forming oxide systems.

Before correlating the enthalpy effects on mixing (Figs. 4, 5) to their structural origin, a short overview of what is known about the structure of the considered melt is given. In this, information provided by structural studies on glasses is taken to describe the structural situation in the corresponding melts. Experimental data to prove the structural similarity between germanate melts and their quenched analogues are comparatively few (e.g. refs. 21 and 22). However, on the basis of Raman and infrared spectra of related glass-forming silicate melts, it can be concluded that there are no remarkable differences between the spectra of glass-forming oxide melts and the corresponding glasses (see, for example, refs. 23 and 24).

There is general agreement that liquid (and vitreous) GeO_2 may best be described as a disordered three-dimensional network which is very similar

to that of hexagonal GeO_2 [25]. Although the details of the structure have not been clarified, it has been established that the network is made up of $GeO_{4/2}$ tetrahedra joined at their corners [21, 26–30]. On addition of Na_2O to an excess of pure liquid (or vitreous) GeO_2, tetrahedral $GeO_{4/2}$ units are converted into octahedral $GeO_{6/2}$ units [31, 32]. For each oxygen added to GeO_2 as Na_2O, one octahedron is produced, without, however, formation of non-bridging oxygens [22, 33–35]. X-ray diffraction studies [22, 34, 36, 37], spectroscopic investigations [33, 34, 38–42], and neutron scattering experiments [35] on sodium germanate glasses have shown that the fraction of six-coordinated germanium atoms appears to increase linearly with decreasing GeO_2 content, and reaches a maximum in the vicinity of $x = 0.80$. At lower GeO_2 contents, the fraction of six-coordinated Ge atoms decreases to become equal to zero at $x \approx 0.65$.

Vibrational spectroscopy, in particular the Raman technique, has provided ample evidence that local coordination in sodium germanate glasses and melts is related to that in the corresponding crystals; this evidence is shown by the similarity in the Raman and infrared spectra of crystals and glasses (see, for example, refs. 39 and 41). The spectrum of glass is much broader but shows similar frequencies associated with bending and stretching vibrations of anionic groups present in both crystal and glass. The groups thus identified exist in specific regions of composition. In the high-GeO_2 range, several different structural units have been found to coexist [39], and it has been proposed that, apart from disordered three-dimensional GeO_2-like structures, anionic species with six-coordinated Ge (without non-bridging oxygens) are present. The latter have been suggested to resemble either the anionic group in the $2Na_2O \cdot 9GeO_2$ crystal [41] or that in the $Na_2O \cdot 4GeO_2$ crystal [34]. There are certain indications in favour of the enneagermanate species which has been described to consist of chains of $GeO_{4/2}$ tetrahedra connected by $GeO_{6/2}$ octahedra [41]. Disordered enneagermanate structures may thus be supposed to predominate in the high-GeO_2 range; and it may then be assumed that these structures possess maximum stability in the region around $x \approx 0.82$. However, the progressive breakdown of the GeO_2 network with decreasing GeO_2 content starts at $x \approx 0.85$ with the formation of the first polymeric units containing non-bridging oxygens [39, 41]. Below $x \approx 0.85$, disordered GeO_5^{2-} sheet-like structures (with one non-bridging oxygen per Ge atom) appear in growing numbers, and around $x \approx 0.67$ the $Ge_2O_5^{2-}$ group prevails. Below this composition, disordered $Ge_2O_6^{4-}$ chain-like structures (containing two non-bridging atoms per germanium atom) are increasingly stabilized, and the relative abundance of these units apparently has a maximum at $x \approx 0.5$. At $x \approx 0.33$, where the enthalpy of mixing curve exhibits a minimum (Fig. 4), depolymerization is brought to a close. In support of this, it is noted that, in the vicinity of this composition, the partial enthalpies (Fig. 5) experience a drastic change which, following

Ostvold and Kleppa [17], may be attributed to an acid–base reaction of the type $GeO_2 + 2O^{2-} = GeO_4^{4-}$. These findings are corroborated by a comparison of liquid Na_2O–GeO_2 mixtures with corresponding silicates. Binary sodium germanate and silicate mixtures possess similar structures below $x \approx 0.6$ [39, 43], and it has been shown that the orthosilicate composition contains mainly isolated $SiO_{4/2}$ tetrahedra [44]. By analogy with the sodium silicate system, it may hence be suggested that, in the germanate system at $x \approx 0.33$, the GeO_4^{4-} anion is the predominant species, and it may further be conjectured that, below $x \approx 0.33$, melts are mainly composed of Na^+, free O^{2-}, and isolated GeO_4^{4-} ions.

The above discussion shows that when pure liquid Na_2O and GeO_2 combine to form germanate melts with compositions in the range $1 < x < 0.7$, the depolymerization of the GeO_2 network according to reactions of the type

$$\equiv Ge–O–Ge\equiv + Na_2 \rightarrow 2(\equiv Ge–O^-Na^+) \quad (4)$$

represents the main structure-forming process. From the results as represented in Figs. 4 and 5, it is inferred that this process proceeds with a decrease in enthalpy, and the question now arises as to which factors in the underlying bond mechanism are responsible for the exothermic enthalpy effects.

The larger electronegativity difference between germanium and oxygen, compared to that between silicon and oxygen, indicates an increased degree of ionic character in the Ge–O bonds. To a crude approximation, the germanate mixtures under discussion can, therefore, be regarded as being governed by an essentially ionic bonding with a covalent contribution, which may be discussed using the concept of polarization. In GeO_2, a bridging oxygen is polarized by two Ge^{4+} ions, while in the germanate melt a non-bridging oxygen is polarized by a single Ge^{4+} ion only; the compartively small polarizing effect of the adjacent Na^+ ion, having a relatively large radius, low charge, and an electron configuration of the noble gas type, may be neglected. Thus, when reaction (4) occurs, a polarized ("bridging") O^{2-} ion of GeO_2 and a weakly deformed ("free") O^{2-} ion of Na_2O form all together two non-bridging oxygens, each of which is unsymmetrically polarized by one Ge^{4+} ion.

These significant changes in the polarization of the oxygen ions concerned may be considered more quantitatively using a model devised by Ramberg [45]. On the basis of this model it is suggested that the enthalpy reduction accompanying reaction (4) may be virtually attributed to the energy release connected with a strengthening of the Ge–O^- bonds. In the considered range of composition, the enthalpy of mixing is therefore reduced with decreasing GeO_2 content because of the growing number of Ge–O^- bonds. In accordance with this, the minimum on the enthalpy of mixing curve appears at $x = 0.33$ where the depolymerization of the GeO_2

network reaches its maximum. Below $x = 0.33$, complete depolymerization continues; the enthalpy of mixing, however, increases with decreasing GeO_2 content due to the increasing "dilution" of GeO_2 in the liquid Na_2O–GeO_2 mixtures.

Concerning the composition range $x \geqslant 0.7$, the findings from the aforementioned structural investigations suggest that two relevant structure-forming processes occur:

(a) Oxygen ions are transferred from the coordination sphere of the Na^+ ions to the coordination with Ge to form $GeO_{6/2}$ octahedra

$$(GeO_{4/2})^0 + Na_2O \rightarrow (GeO_{6/2})^{2-} + 2Na^+$$

(b) At least part of the octahedral units join, along with remaining tetrahedral units, to build up discrete anionic groups, e.g. the above-mentioned enneagermanate species, the excess electric charge of which is compensated by the incorporation of the corresponding number of sodium ions. These small regions of local order may be assumed to be randomly dispersed throughout the persisting polymerized structure of the germanate melt.

According to the data represented in Fig. 4, the overall energy effect accompanying processes (a) and (b) is exothermic in nature, whereas process (a), due to its connection with the transition of the Ge–O bond from sp^3 to d^2sp^3 hybridization, is supposed to be associated with absorption of energy. Process (b) may then be assumed to proceed with release of energy. Obviously, these assumptions, being most speculative, require confirmation by further investigations using pertinent methods.

ACKNOWLEDGEMENT

The authors are indebted to Professor M. Hoch, Cincinnati, for comments on the manscript.

REFERENCES

1 J. Klein and F. Müler, High Temp. High Press., 19 (1987) 201.
2 F. Müller and S. Demirok, Glastech. Ber., 62 (1989) 142.
3 R. Schwarz and F. Heinrich, Z. Anorg. Allg. Chem., 205(1) (1932) 43.
4 S.G. Tresvyatskii, Dopov. Akad. Nauk Ukr. RSR, 3 (1958) 295.
5 M.K. Murthy and J. Aguayo, J. Am. Ceram. Soc., 47(9) (1964) 444.
6 B. Monnaye, Rev. Chim. Miner., 12 (1975) 268.
7 R. Ota, H. Tashíro and N. Soga, Yogyo Kyokai Shi, 94(2) (1986) 249.
8 S. Kohsaka, S. Sato and T. Yokokawa, J. Chem. Thermodyn., 10 (1978) 117.
9 M.M. Shul'ts, V.L. Stolyarova and G.A. Semenov, J. Non-Cryst. Solids, 38/39 (1980) 581.
10 W. Wilsmann and F. Müller, Thermochim. Acta, 151 (1989) 309.
11 K.K. Kelley, U.S. Bur. Mines Bulletin, No. 584, U.S. Government Printing Office, Washington, D.C., 1960.

12 E. Zintl and H.H. von Baumbach, Z. Anorg. Allg. Chem., 198 (1931) 88.
13 I. Barin and O. Knacke, Thermochemical properties of Inorganic Substances, Springer-Verlag, Berlin, 1973.
14 J.L. Holm and O.J. Kleppa, Inorg. Chem., 8 (1969) 207.
15 R.H. Rein and J. Chipman, Trans. Metall. Soc. AIME, 233 (1965) 415.
16 R.J. Charles, Phys. Chem. Glasses, 10 (1969) 169.
17 T. Ostvold and O.J. Kleppa, Inorg. Chem., 8 (1969) 78.
18 J.L. Holm and O.J. Kleppa, Inorg. Chem., 6 (1967) 645.
19 M.K. Murthy and J. Ip, J. Am. Ceram. Soc., 47 (1964) 328.
20 M.K. Murthy, L. Long and J. Ip, J. Am. Ceram. Soc., 51 (1968) 661.
21 J. Zarzycki, Verres Refract., 11 (1957) 3.
22 K. Kamiya, T. Yoko, Y. Itoh, and S. Sakka, J. Non-Cryst. Solids, 79 (1986) 285.
23 J.R. Sweet and W.B. White, Phys. Chem. Glasses, 10 (1969) 246.
24 S.K. Sharma, D. Virgo and B.O. Mysen, Carnegie Inst. Washington Yearb., 77 (1978) 649.
25 J. Wong and C.A. Angell, Glass Structure by Spectroscopy, Marcel Dekker, New York and Basel, 1963.
26 E. Lorch, J. Phys. C, 2 (1969) 229.
27 G.A. Ferguson and M. Hass, J. Am. Ceram. Soc., 53 (1970) 109.
28 A.J. Leadbetter and A.C. Wright, J. Non-Cryst. Solids, 7 (1972) 37.
29 W.F. Nelson, I. Siegel and R.W. Wagner, Phys. Rev., 127 (1962) 2025.
30 V.A. Tyul'kin and N.I. Shalunenko, Izv. Akad. Nauk SSSR, Neorg. Mater., 7(12) (1971) 2203.
31 A.D. Ivanov and K.S. Yestropiev, Dokl. Akad. Nauk SSSR, 145 (1962) 797.
32 M.K. Murthy and J. Ip, Nature (London), 201 (1964) 285.
33 S. Sakka and K. Kamiya, Rev. Chim. Miner., 16 (1979) 293.
34 S. Sakka and K. Kamiya, J. Non-Cryst. Solids, 49 (1982) 103.
35 M. Ueno, M. Misawa and K. Suzuki, Physica B, 120L (1983) 347.
36 N. Iwamoto and N. Umesaki, Nippon Kinzoku Gakkaishi, 42 (1978) 857.
37 K. Kamiya and S. Sakka, Phys. Chem. Glasses, 20 (1979) 60.
38 M.K. Murthy and E.M. Kirby, Phys. Chem. Glasses, 5 (1964) 144.
39 T. Furukawa and W.B. White, J. Mater. Sci., 15 (1980) 1648.
40 S. Sakka, K. Kamiya and M. Hayashi, Bull. Inst. Chem. Res. Kyoto Univ., 59 (1981) 172.
41 H. Verweij and J.H.J.M. Buster, J. Non-Cryst. Solids, 34 (1979) 81.
42 M. Tada, F. Marumo, H. Oyanagi and S. Hosoya, Yogyo Kyokai Shi, 90 (1982) 247.
43 E.F. Riebling, J. Chem. Phys., 39 (1963) 3022.
44 Y. Waseda and J.M. Toguri, Metall. Trans., 9B (1978) 595.
45 H. Ramberg, Am. Mineral., 39 (1954) 256.